TABLE 1
Protein symbols of protrudin-associated proteins categorized in terms of subcellular localization

Subcellular localization	Protein symbol																													
Plasma membrane	ASPH	ATP1A1	ATP1A2	ATP1A3	ATP1B1	ATP1B2	ATP2B1	ATP2B2	ATP2B4	ATP5A1	ATP5B	CDC42	DPP6	GNA11	GNA13	GNAI1	GNAI2	GNAO1	GNAQ	GNB1	GNB2	GPM6A	GPR37L1	GRIA2	HK1	HMOX2	LPHN1	NCAM1	NLGN2	NLGN3
	NSF	OPALIN	P2RY12	PRKACA	PRKAC8	PRKAR2B	RAB10	RAB2B	RAB39B	RAB3A	RAB3B	RAB3GAP2	RTN4	SCAMP5	SEPT5	SLC1A3	SLC1A2	SLC3A2	SLC9A11	SNAP25	SORT1	SYNGR1	SYNGR3	VAPA	ZFYVE27					
Endoplasmic reticulum	ASPH	ATL1	ATP1A1	ATP1A3	ATP2A1	ATP2A2	ATP2B2	CANX	CD52	CPT1C	CYP4B1	ERP44	FAAH	GRIA2	HMOX2	LPCAT4	NCEH1	PGRMC1	PLD3	PTPLAD1	RAB2B	RCN2	RTN1	RTN3	RTN4	SORT1	SURF4	VAPA	VAPB	ZFYVE27
Golgi apparatus	ATL1	ATP1A1	ATP1A3	CDC42	COPB2	COPG2	FAAH	MAP6D1	NSF	OPALIN	PRKACA	RAB10	RAB2B	RAB33B	RAB39B	RABEA	RTN3	SCAMP5	SLC1A6	SNAP25	SORT1	SURF4	VAPB							
Mitochondrion	ACAT1	ATP5A1	ATP5B	ATP5C1	ATP5F1	BDH1	BRI3BP	C1QBP	CCDC136	CD52	CPT1C	GAD1	GPX4	HK1	HSPA9	MFN1	P2RY12	PPP2CA	PRKACA	PRKAR2B	SDHA	SLC1A3	SLC25A22	TMM50	YWHAE	YWHAZ				
Cytoskeleton	ARL8A	CDC42	COPB2	GNAI1	GNAI2	GRIA2	KIF5A	KIF5B	KIF5C	LPHN1	MAP6D1	NSF	PRKACA	PRKACB	PRKAR2B	SEPT5	SNAP25	TUBAL3	VAPA	YWHAE	YWHAZ									
Cytoplasmic vesicle	CDC42	COPB2	COPG2	GRIA2	MAP6D1	NLGN3	RAB2A	RAB3B	RAB6A	SCAMP5	SEPT5	SORT1	SYNGR1	SYP																
Endosome	ARL8A	ATP1A1	ATP1A2	SCAMP5	SNAP25	SORT1	TMEM55A	ZFYVE27	RAB3B	RAB6A	RPS5																			
Cytosol	DNAJA2	GNAI1	GNAI2	GNAQ	GPX4	HK1	NCDN	PPP3CA																						
Centrosome	GNAI1	GNAI2	PRKACA	PRKAC8	PRKAR2B																									
Lysosome	ARL8A	SORT1	TMEM55A																											
Ribosome	CANX	RPS5																												
Nucleus	ATP1A2	BDH1	C1QBP	DNAJA2	GNAI1	GNAI2	GNAQ	GPX4	HK1	HSPA8	NCDN	PGRMC1	PPP3CA	PRKACA	PRKACB	PURA	RTN4	SLC25A22	SORT1	TMM50	YWHAZ									
Nuclear lumen	PGRMC1	PURA	TMM50																											

TABLE 2
Responsible genes for HSP, ALS, Charcot-Marie-Tooth disease (CMT), Parkinson disease (PD), and spinocerebellar ataxia (SCA)

Gene symbols of protrudin-associated proteins identified by proteomics analysis were represented in bold.

HSP	ALS	CMT	PD	SCA
AP4B1	*ALS2*	*AARS*	*ADH1C*	*AFG3L2*
AP4E1	*ANG*	*AIFM1*	*ATP13A2*	*ATXN1*
AP4M1	*ATXN2*	*ARHGEF10*	*EIF4G1*	*ATXN10*
AP4S1	*C9ORF72*	*BSCL2*	*FBXO7*	*ATXN2*
AP5Z1	*CHMP2B*	*DNM2*	*GBA*	*ATXN3*
ATL1	*DAO*	*DYNC1H1*	*GIGYF2*	*ATXN7*
BSCL2	*DCTN1*	*EGR2*	*HTRA2*	*CACNA1A*
C12orf65	*FIG4*	*FGD4*	*LRRK2*	*FGF14*
CYP2U1	*FUS*	*FIG4*	*MAPT*	*ITPR1*
CYP7B1	*NEFH*	*GARS*	*PARK2*	*KCNC3*
DDHD1	*OPTN*	*GDAP1*	*PARK7*	*KCND3*
DDHD2	*PRPH*	*GJB1*	*PINK1*	*KLHL1*
ERLIN2	*SETX*	***HK1***	*PLA2G6*	*NOP56*
FA2H	*SIGMAR1*	*HSPB1*	*SNCA*	*PDYN*
GJC2	*SOD1*	*HSPB8*	*TBP*	*PPP2R2B*
HSPD1	*SPG11*	*KARS*	*UCHL1*	*PRKCG*
KIAA0196	*TAF15*	*KIF1B*	*VPS35*	*SPTBN2*
KIF1A	*TARDBP*	*LITAF*		*TBP*
KIF5A	*UBQLN2*	*LMNA*		*TGM6*
L1CAM	***VAPB***	*LRSAM1*		*TK2*
NIPA1	*VCP*	*MED25*		*TTBK2*
PGN		*MFN2*		
PLP1		*MPZ*		
PNPLA6		*MTMR2*		
REEP1		*NAMSD*		
RTN2		*NDRG1*		
SLC16A2		*NEFL*		
SLC33A1		*PMP22*		
SPAST		*PRPS1*		
SPG11		*PRX*		
SPG20		*RAB7A*		
SPG21		*SBF2*		
TECPR2		*SH3TC2*		
VPS37A		*TRPV4*		
ZFYVE26		*YARS*		
ZFYVE27				

transfected with an expression vector encoding mouse protrudin tagged with the HA epitope at its NH_2 terminus and with the Myc epitope at its COOH terminus (HA-protrudin-Myc), and cell lysates were subjected to alkaline extraction with sodium carbonate. Immunoblot analysis revealed that protrudin was resistant to such extraction, as was the integral membrane protein calnexin, whereas the membrane-attached protein GM130 was extracted into the supernatant (Fig. 3*B*), suggesting that protrudin is an authentic integral membrane protein.

Protrudin Contains a Hydrophobic Hairpin Domain—Other HSP-related proteins found to associate with protrudin, including reticulon family members, atlastin-1, REEP5, and REEP1, contain hydrophobic hairpin domains. Given that these domains affect ER morphology by shaping the lipid bilayer into high-curvature tubules, we investigated whether protrudin also contains such sequences. We examined the membrane topology of protrudin with two approaches. First, we subjected a membrane fraction prepared from cells expressing HA-protrudin-Myc to protease treatment. As a control, we confirmed that the NH_2 terminus of calnexin, which faces the luminal side of the ER, was protected from proteolytic attack, whereas the COOH terminus of this protein, which is exposed to the cytosolic side, was cleaved (Fig. 4, *A* and *B*). In contrast, both the NH_2 and COOH termini of HA-protrudin-Myc were completely processed by treatment with proteinase K (Fig. 4*B*), suggesting that both termini of the protein are exposed to the cytosol. These results thus raised the

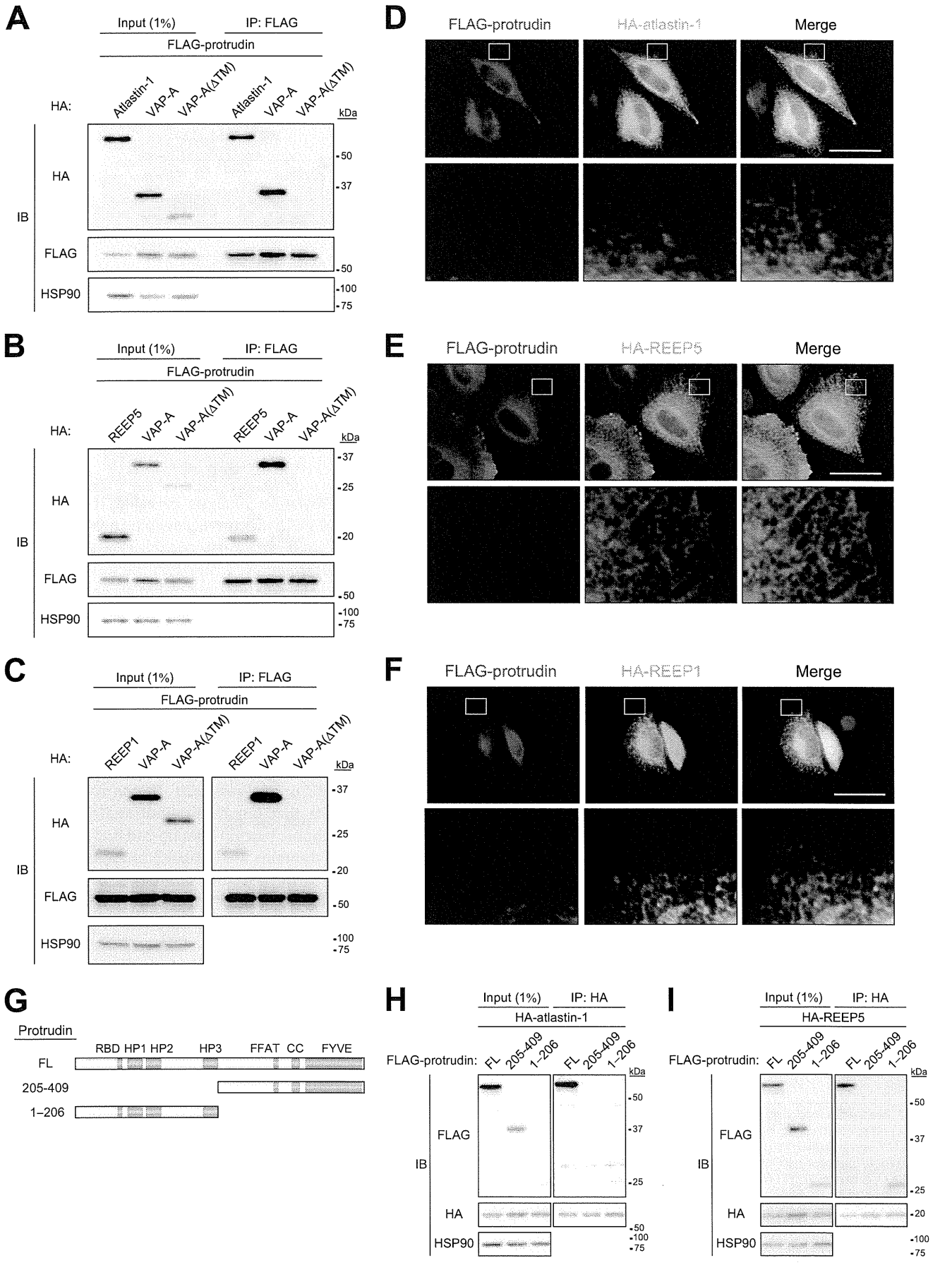
A
Input (1%)
IP: FLAG
FLAG-protrudin
HA:
Atlastin-1
VAP-A
VAP-A(ΔTM)
kDa
IB
HA
FLAG
HSP90
50
37
100
75
B
REEP5
C
REEP1
D
FLAG-protrudin
HA-atlastin-1
Merge
E
HA-REEP5
F
HA-REEP1
G
Protrudin
RBD HP1 HP2
HP3
FFAT CC
FYVE
FL
205-409
1–206
H
Input (1%)
IP: HA
HA-atlastin-1
FLAG-protrudin:
I
HA-REEP5

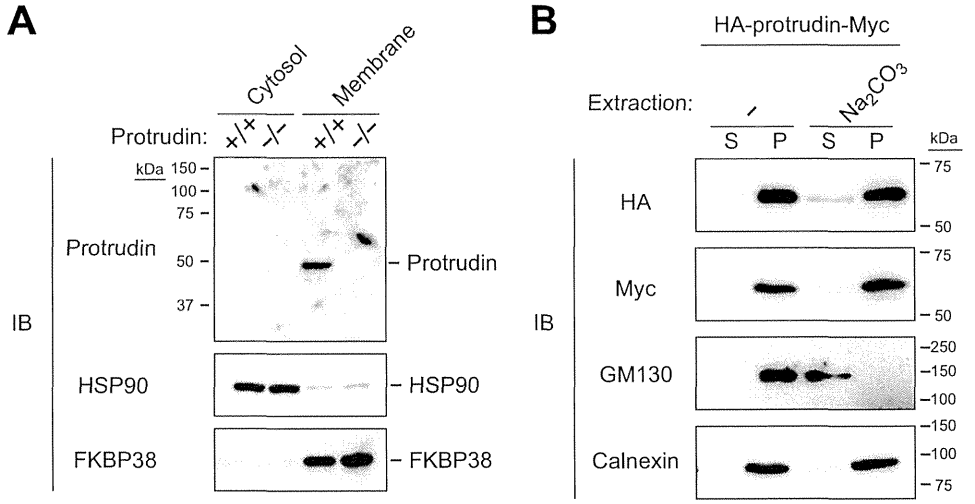

FIGURE 3. **Protrudin is an integral membrane protein.** *A*, cytosolic and membrane fractions were isolated from the brain of WT (+/+) or protrudin-deficient (−/−) mice, and equal amounts of protein from each fraction were subjected to immunoblot analysis with anti-protrudin, anti-HSP90, and anti-FKBP38. HSP90 and FKBP38 were examined as controls for cytosolic and membrane proteins, respectively. *B*, homogenates of HEK293T cells expressing protrudin tagged at its NH_2 and COOH termini with HA and Myc epitopes, respectively, were subjected to extraction with or without Na_2CO_3 followed by centrifugation to isolate supernatant (*S*) and pellet (*P*) fractions. Equal amounts of protein from each fraction were subjected to immunoblot analysis with anti-HA, anti-Myc, anti-GM130, and anti-calnexin. GM130 and calnexin were examined as controls for peripheral and integral membrane proteins, respectively.

question of whether the three hydrophobic regions (HP1 to HP3) present in protrudin span the entire membrane or are buried within the phospholipid bilayer. To determine the membrane topology around the hydrophobic regions of protrudin, we subjected a deletion mutant of HA-protrudin-Myc to the same analysis. The region between HP2 and HP3 (examined with the mutant 1–188) was cleaved by the protease, suggesting that this region is exposed to the cytosol (Fig. 4*C*).

As a second approach, we performed a PEGylation assay, which is based on the premise that cysteine residues in the cytosolic region of an ER protein, but not those in the luminal region or within the phospholipid bilayer, are accessible to mPEG. Cysteine residues are present at positions 72, 77, 113, 169, 172, 199, and 207 in the region of mouse protrudin spanning HP1 to HP3 (Fig. 4*D*). Calnexin, which contains one cysteine residue in the cytosolic portion and five cysteines in the luminal portion of the protein, showed one and three band shifts after PEGylation in the absence or presence of ER membrane permeabilization, respectively (Fig. 4*E*). To identify the accessible cysteine residues around the hydrophobic regions of protrudin, we generated a series of mutant proteins by inserting a cysteine-containing sequence (GGCGG or GGECEGG) between residues 87 and 88 in the region between HP1 and HP2, or by replacing the cysteines at positions 113, 169, and 172 in the region between HP2 and HP3 with alanine, in combination with replacement of the cysteine at position 25 (Fig. 4, *A* and *D*). The PEGylation analysis revealed that the region between HP1 and HP2 was not accessible to mPEG, whereas that between HP2 and HP3 was accessible (Fig. 4*F*), suggesting that the region between HP1 and HP2 faces the ER lumen, although this sequence is short and might be present to a variable extent within the membrane. Although we are unable to exclude the possibility that the overexpressed tagged proteins do not necessarily reflect the topology of endogenous protrudin, the results of our two approaches (protease protection assay and mPEG modification assay) together suggested that HP1 and HP2 domains span the membrane fully, with the loop between HP1 and HP2 residing in the ER lumen, and that the HP3 domain folds into a hairpin.

Forced Expression of Protrudin Promotes ER Network Formation—Given that our results indicated that protrudin contains a hydrophobic hairpin domain and that many proteins that possess such domains are localized to the tubular ER network, we examined in more detail whether protrudin might also reside in tubular ER as opposed to sheetlike ER. To this end, we compared the intracellular localization of protrudin with those of Climp63 and REEP5, which largely reside in sheetlike and tubular ER, respectively (20). Immunofluorescence analysis revealed that FLAG-tagged protrudin did not colocalize with enhanced green fluorescent protein (EGFP)-tagged Climp63 in COS-7 cells, whereas the distribution of FLAG-protrudin was almost identical to that of HA-REEP5 (Fig. 5, *A–C*). We also

FIGURE 2. **Protrudin interacts with atlastin-1 and REEP family members.** *A–C*, extracts of HEK293T cells transiently transfected with expression vectors for FLAG-tagged protrudin and HA epitope-tagged forms of atlastin-1, REEP5, or REEP1 were subjected to immunoprecipitation (*IP*) with anti-FLAG. VAP-A and VAP-A(ΔTM) were studied as positive and negative controls, respectively, for interaction with protrudin. The resulting precipitates, as well as a portion (1% of the input for immunoprecipitation) of the cell extracts, were subjected to immunoblot (*IB*) analysis with anti-HA, anti-FLAG, and anti-HSP90 (loading control). *D–F*, HeLa cells expressing FLAG-tagged protrudin and HA epitope-tagged forms of atlastin-1, REEP5, or REEP1 were fixed and processed for immunofluorescence analysis with anti-FLAG (*red*) and anti-HA (*green*). Merged images in which nuclei are stained with Hoechst 33258 (*blue*) are also shown. The *boxed areas in the upper panels* are shown at higher magnification in the *lower panels*. *Scale bars*, 50 μm. *G*, domain organization of human protrudin and structure of deletion mutants thereof. *RBD*, Rab binding domain; *HP1* to *HP3*, hydrophobic domains; *CC*, coiled-coil domain. *H* and *I*, extracts of HEK293T cells expressing full-length (*FL*) protrudin or its mutants shown in *G* (fused at their NH_2 termini to the FLAG tag) together with HA-atlastin-1 (*H*) or HA-REEP5 (*I*) were subjected to immunoprecipitation with anti-HA, and the resulting precipitates, as well as a portion (1% of the input for immunoprecipitation) of the cell extracts, were subjected to immunoblot analysis with anti-FLAG, anti-HA, and anti-HSP90.

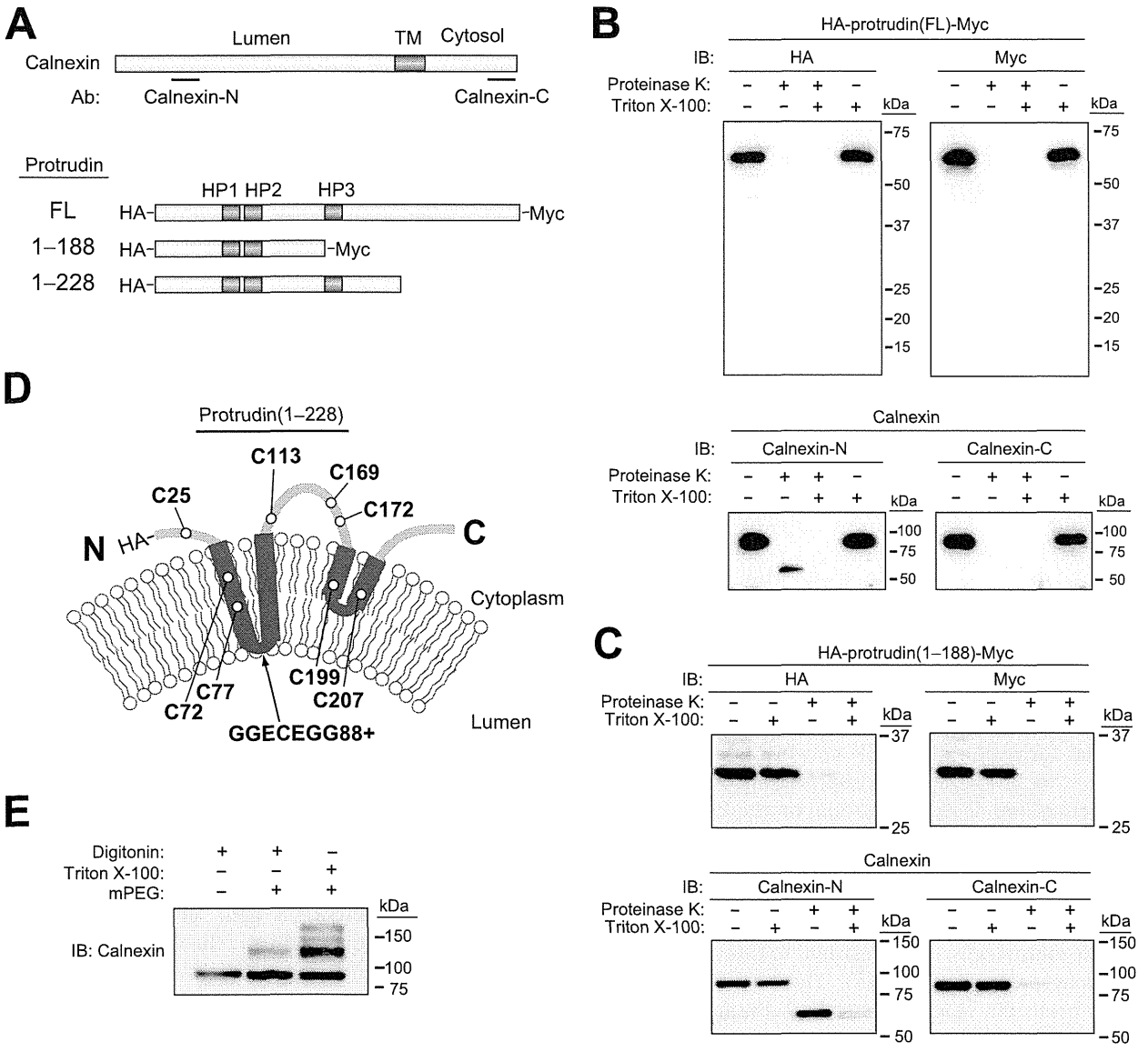
A
Lumen
TM
Cytosol
Calnexin
Ab:
Calnexin-N
Calnexin-C
Protrudin
HP1 HP2 HP3
FL
HA-
-Myc
1–188
1–228
B
HA-protrudin(FL)-Myc
IB:
HA
Myc
Proteinase K:
Triton X-100:
kDa
Calnexin
Calnexin-N
Calnexin-C
C
HA-protrudin(1–188)-Myc
D
Protrudin(1–228)
C113
C169
C25
C172
N
HA-
C
Cytoplasm
C77
C72
C199
C207
GGECEGG88+
Lumen
E
Digitonin:
Triton X-100:
mPEG:
IB: Calnexin
F
HA-protrudin(1–228):
WT
(C72A, C77A)
(GGCGG88+)
(C113A, C169A, C172A)
(C25A)
(C25A, C113A, C169A, C172A)
(C25A, GGECEGG88+)
IB
HA
Calnexin

examined the potential colocalization of FLAG-protrudin with endogenous Climp63 (Fig. 5*D*) and calreticulin (a marker for all of the ER) (Fig. 5*E*). The extent of colocalization between FLAG-protrudin and endogenous Climp63 was markedly lower than that between FLAG-protrudin and endogenous calreticulin (Fig. 5*F*). These results suggested that protrudin is predominantly localized to the tubular ER.

Given that we found that protrudin interacts with atlastin-1, a dynamin-like GTPase that promotes ER network formation through homotypic membrane fusion of ER tubules (9, 10, 21, 22), we investigated whether protrudin also promotes ER network formation. The reticular mesh of the ER network (as revealed by immunofluorescence analysis of calreticulin) became finer and more complex, as reflected by an increase in the density of three-way junctions especially at the cell periphery, as a result of overexpression of protrudin (Fig. 5, *E* and *G*). These results indicated that protrudin may promote the fusion of ER tubules and ER network formation. We also found that depletion of protrudin by RNAi in HeLa cells (Fig. 5*H*) rendered the sheetlike structure of the ER more prominent (Fig. 5, *I* and *J*). Expression of FLAG-protrudin in such protrudin-depleted HeLa cells resulted in reversion of the morphology of the ER to a pattern similar to that observed in control cells, suggesting that protrudin indeed contributes to regulation of the sheet *versus* tubule structure of this organelle.

Given that formation of the ER network is dependent on microtubules, we investigated the effects of nocodazole, which induces microtubule depolymerization, on the ER network in cells transfected with a vector for FLAG-protrudin or with the corresponding empty vector. Whereas the ER network (as revealed by the fluorescence of a tdTomato-tagged form of the ER protein Sec61β) disappeared in response to nocodazole treatment in control cells, it was resistant to this agent in those overexpressing protrudin (Fig. 5*K*). These results thus suggested that protrudin contributes to both the formation and stabilization of the tubular ER network.

Cells Expressing Mutant Protrudin Are Susceptible to ER Stress—We next examined whether protrudin(G191V), which has been identified in a subset of HSP patients, also interacts with atlastin-1, REEP5, and REEP1. The interaction between protrudin and each of these three proteins was not affected by the G191V mutation (Fig. 6, *A–C*). We also examined the localization of FLAG-protrudin(G191V) in COS-7 cells by immunofluorescence analysis. The distribution of the mutant protein did not differ substantially from that of WT protrudin (Fig. 6*D*), suggesting that the pathogenesis of HSP associated with this mutation of protrudin is not attributable to a change in the subcellular localization of the protein. Aggregate formation by the mutant protein was also not apparent, at least at the level of resolution achieved with the light microscope used for immunofluorescence analysis. Furthermore, forced expression of protrudin(G191V) induced a change in ER morphology similar to that induced by overexpression of the WT protein in COS-7 cells, and it resulted in stabilization of the ER network in a manner similar to that apparent with WT protrudin in cells treated with nocodazole (Fig. 6*E*). We therefore conclude that the HSP-associated G191V mutation of protrudin affects neither the localization of the protein nor its function in the regulation of ER morphology and stability.

Impairment of ER function may result in abnormal accumulation of unfolded or misfolded proteins, a condition referred to as ER stress. Mutations in some SPG genes, such as *SPG17* (23), have been shown to result in misfolding and aggregation of the encoded proteins, which triggers ER stress and may play a role in HSP pathogenesis. We therefore examined the effect of protrudin mutation on the ER stress response. Forced expression of WT human protrudin did not affect the increase in the amount of mRNA for the ER stress-inducible gene *Bip* (also known as *Grp78*) elicited by exposure of Neuro2A cells to ER stress-inducing agents such as tunicamycin, thapsigargin, and DTT. However, expression of the HSP-associated protrudin(G191V) mutant enhanced the *Bip* gene response to all three agents (Fig. 7, *A–C*). We also examined whether cells expressing protrudin(G191V) manifest ER stress with the use of an ER stress response element reporter assay and by monitoring the splicing of *Xbp1* mRNA. Neuro2A cells infected with retroviruses encoding WT or G191V mutant forms of protrudin were transfected with a luciferase reporter vector under the control of the *BIP/GRP78* gene promoter. Expression of protrudin(G191V), but not that of the WT protein, resulted in a moderate but significant increase in luciferase activity compared with that of control cells (Fig. 7*D*), suggestive of the presence of ER stress triggered by expression of the mutant protein even in the absence of an ER stress-inducing agent. We also examined the splicing of *Xbp1* mRNA in cells expressing WT or mutant protrudin in the absence or presence of tunicamycin treatment. Whereas the spliced form of *Xbp1* mRNA was essentially undetectable in cells not exposed to tunicamycin, this drug increased the amount of the spliced mRNA to a greater extent in cells expressing the G191V mutant than in those expressing WT protrudin (Fig. 7*E*). On the basis of these results, we speculate that the relatively modest effect of protrudin(G191V) on ER stress might accumulate over long periods of time (decades) before the onset of symptoms in indi-

FIGURE 4. **Analysis of the membrane topology of protrudin.** *A*, schematic representation of calnexin as well as full-length (*FL*) and mutant forms of mouse protrudin. The transmembrane (*TM*) domain of calnexin as well as the hydrophobic regions (*HP1* to *HP3*) of protrudin are indicated. NH_2- or COOH-terminal epitopes recognized by anti-calnexin (calnexin-N and calnexin-C, respectively) are denoted by *black bars*. Full-length and mutant forms of protrudin were tagged at their NH_2 and COOH termini with HA and Myc epitopes, respectively, as indicated. *B*, microsomes prepared from HEK293T cells expressing full-length HA-protrudin-Myc were incubated in the absence or presence of proteinase K and Triton X-100 and then subjected to immunoblot analysis with anti-HA, anti-Myc, anti-calnexin-N, or anti-calnexin-C, as indicated. *C*, microsomes prepared from HEK293T cells expressing HA-protrudin-(1–188)-Myc were analyzed as in *B*. *D*, schematic representation of the topology of HA epitope-tagged protrudin mutants. *E*, HeLa cells were incubated with digitonin to permeabilize the plasma membrane or with Triton X-100 to permeabilize all cell membranes. They were then treated with or without mPEG and subjected to immunoblot analysis with anti-calnexin. *F*, cysteine residues of protrudin-(1–228) were mutated to alanine, or sequences GGCGG or GGECEGG were inserted before residue 88, as indicated in *D*. HeLa cells expressing the various HA epitope-tagged protrudin mutants were then analyzed as in *E* with the exception that immunoblot analysis was performed with anti-HA and anti-calnexin.

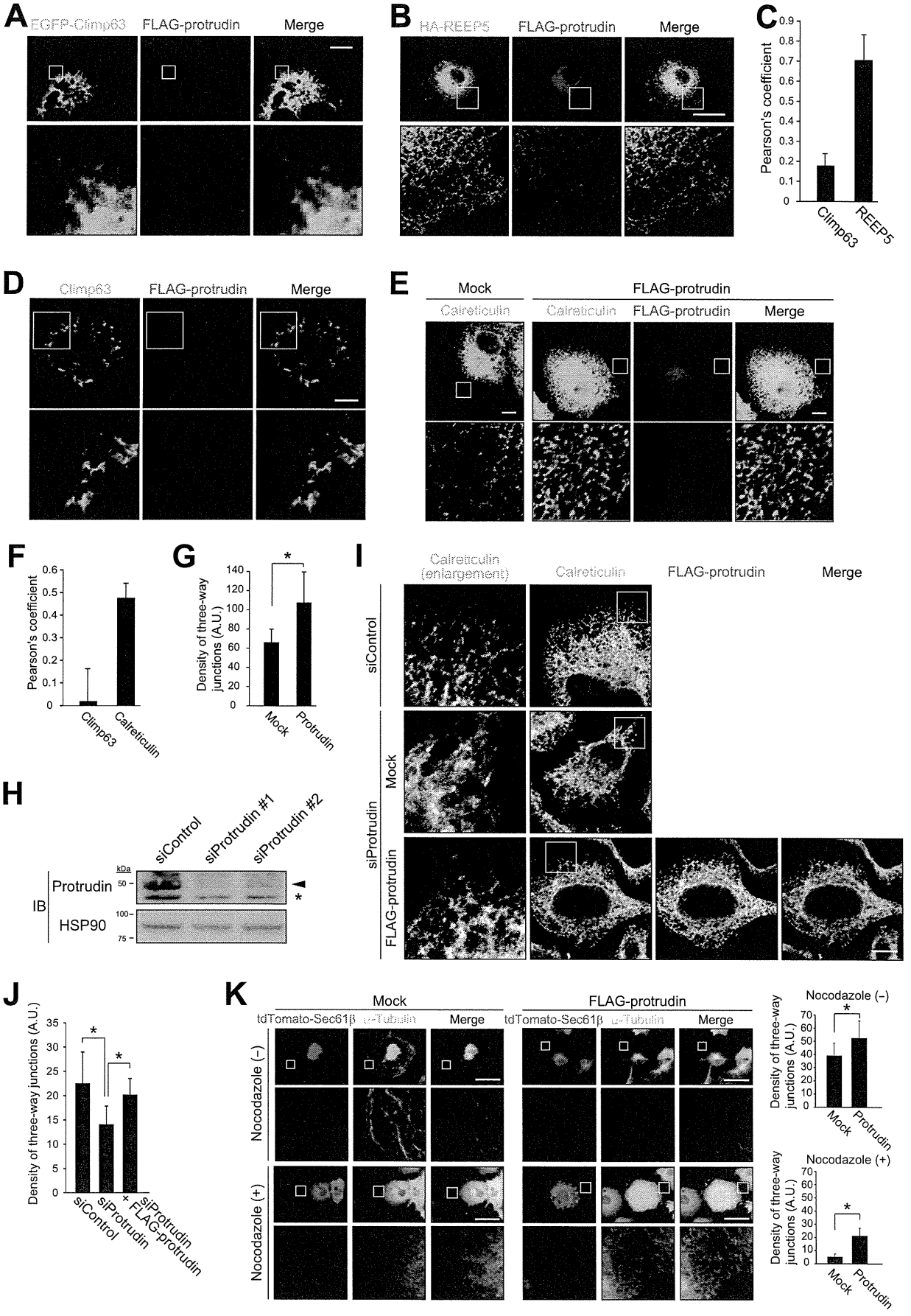
A
EGFP-Climp63
FLAG-protrudin
Merge
B
HA-REEP5
FLAG-protrudin
Merge
C
Pearson's coefficient
Climp63
REEP5
D
Climp63
FLAG-protrudin
Merge
E
Mock
FLAG-protrudin
Calreticulin
Calreticulin
FLAG-protrudin
Merge
F
Pearson's coefficient
Climp63
Calreticulin
G
Density of three-way junctions (A.U.)
Mock
Protrudin
H
siControl
siProtrudin #1
siProtrudin #2
kDa
Protrudin
HSP90
IB
I
Calreticulin (enlargement)
Calreticulin
FLAG-protrudin
Merge
siControl
siProtrudin
Mock
FLAG-protrudin
J
Density of three-way junctions (A.U.)
siControl
siProtrudin
siProtrudin + FLAG-protrudin
K
Mock
FLAG-protrudin
tdTomato-Sec61β
α-Tubulin
Merge
Nocodazole (−)
Nocodazole (+)
Density of three-way junctions (A.U.)
Mock
Protrudin

viduals with HSP, similar to the long time courses for the development of other human neurodegenerative diseases.

Some SPG proteins have been functionally linked to ER-associated degradation (ERAD), a multistep pathway encompassing the degradation of ER proteins by the ubiquitin-proteasome system. We therefore examined the relationship of ERAD to the mutation of protrudin. The half-life of protrudin(G191V) in Neuro2A cells was markedly longer than that of protrudin(WT) (Fig. 7*F*), suggesting that the HSP-associated mutation of protrudin may result in a defect in the ERAD system. Consistent with this observation, the degradation of NHK, a typical substrate of the ERAD system, was delayed in cells expressing protrudin(G191V) compared with that in cells expressing the WT protein (Fig. 7*G*). Furthermore, exposure of cells to the proteasome inhibitor MG132 resulted in partial attenuation of the degradation of WT protrudin to an extent similar to that apparent for cyclin D1 (a soluble proteasome substrate), whereas MG132 almost completely blocked the degradation of protrudin(G191V) (Fig. 7*H*), suggesting that degradation of the mutant protein is highly sensitive to proteasome inhibition. The subcellular localization of the WT and G191V mutant forms of protrudin was not affected by MG132 treatment (data not shown). Given that excessive accumulation of unfolded protein in the ER leads to the UPR or ER overload response, the protrudin(G191V) mutant might be misfolded in the ER, leading to a defect in the ERAD system that enhances the ER stress response. Consistent with this notion, gel filtration analysis revealed that the apparent molecular size of protrudin(G191V) in Neuro2A cells was larger than that of the WT protein (Fig. 7*I*), suggesting that the mutant protein was part of a larger complex. Collectively, these results indicated that mutant protrudin produced in certain individuals with HSP may be prone to aggregation and tend to increase ER stress, which may account for the pathogenesis of HSP.

DISCUSSION

Protrudin is categorized as an HSP-associated protein (SPG33). The relationship between protrudin mutation and HSP pathogenesis has remained largely unclear, however, mainly because (i) the number of HSP patients harboring protrudin mutations is much smaller than that of those with mutations in other SPG genes, such as those for atlastin-1 (SPG3A), spastin (SPG4), and REEP1 (SPG31); (ii) the molecular function of protrudin has not been fully elucidated; and (iii) the mechanism by which the mutation of protrudin affects cell function associated with HSP etiology has been unknown. We recently applied a proteomics approach to Neuro2A cells and found that protrudin associates with Kif5A (SPG10), -B, and -C, and that this interaction is required for the function of protrudin in neurite extension (17). In the present study, we sought to identify molecules that interact with protrudin in mouse brain, a more physiologically relevant system than Neuro2A cells. With this and other approaches, we have now obtained several lines of evidence for a causative relationship between mutation of protrudin and HSP.

First, we found that protrudin interacts with other HSP-related proteins including PLP1 (SPG2), atlastin-1 (SPG3A), REEP1 (SPG31), REEP5 (similar to REEP1), Kif5A (SPG10), Kif5B, Kif5C, and reticulon 1, 3, and 4 (similar to reticulon 2, SPG12). Although we did not detect spastin (SPG4) in the protrudin complexes isolated from mouse brain, others have demonstrated an interaction between protrudin and spastin (14, 24, 25).

Second, many of the HSP-related proteins found to interact with protrudin are thought to contribute to regulation of the morphology of the ER, a heterogeneous organelle with distinct morphologies of sheets and an interconnected network of tubules that share a common lumen. These proteins generate membrane curvature through scaffolding and hydrophobic insertion mechanisms and thereby shape the lipid bilayer of the ER into tubules, resulting in the formation of the tubular ER network (11). The HSP-related proteins possess long hydrophobic stretches of amino acids that form intramembrane hairpin domains and are thought to partially span the lipid bilayer, inducing or stabilizing the high curvature of ER tubules via hydrophobic wedging (12, 26). Depletion of atlastin-1 in cultured cortical neurons was found to inhibit axon elongation (27), and proper ER morphology is thought to be essential for maintenance of long cellular processes such as axons (3). Defects in tubular ER shaping and in interactions of the ER network with the microtubule cytoskeleton thus appear to be

FIGURE 5. **Forced expression of protrudin promotes ER network formation.** *A*, COS-7 cells expressing EGFP-tagged Climp63 and FLAG-tagged human protrudin were fixed and processed for immunofluorescence analysis with anti-FLAG (*red*) and confocal microscopy. The fluorescence of EGFP was monitored directly. Merged images are also shown. The *boxed regions of the upper panels* are shown at higher magnification in the *lower panels*. *Scale bar*, 10 μm. *B*, COS-7 cells expressing HA epitope-tagged REEP5 and FLAG-tagged human protrudin were fixed and processed for confocal immunofluorescence analysis with anti-HA (*green*) and anti-FLAG (*red*). *Scale bar*, 50 μm. *C*, percentage colocalization of FLAG-protrudin with EGFP-Climp63 or HA-REEP5 as determined in *A* and *B* and as measured with Pearson's correlation coefficient in a square area of 2000 μm^2. Data are mean ± S.D. from four or five cells. *D*, COS-7 cells expressing FLAG-tagged human protrudin were fixed and processed for confocal immunofluorescence analysis with anti-Climp63 (*green*) and anti-FLAG (*red*). *Scale bar*, 10 μm. *E*, COS-7 cells transfected with an expression vector for FLAG-tagged human protrudin (or with the corresponding empty vector, *Mock*) were fixed and processed for confocal immunofluorescence analysis with anti-calreticulin (*green*) and anti-FLAG (*red*). *Scale bars*, 10 μm. *F*, percentage colocalization of FLAG-protrudin with Climp63 or calreticulin as determined in *D* and *E* and as measured with Pearson's correlation coefficient in a square area of 2000 μm^2. Data are mean ± S.D. for three cells. *G*, density of three-way junctions of the ER for cells examined as in *E*. Data are mean ± S.D. for five cells. *A.U.*, arbitrary units. *, $p < 0.05$ (Student's *t* test). *H*, HeLa cells transfected with protrudin or control siRNAs were subjected to immunoblot analysis with anti-protrudin and anti-HSP90. The *arrowhead* and *asterisk* indicate specific and nonspecific bands, respectively. *I*, HeLa cells transfected with protrudin or control siRNAs were subsequently transfected with an expression vector for FLAG-tagged human protrudin (or with the corresponding empty vector, Mock) before fixation and processing for confocal immunofluorescence analysis with anti-calreticulin (*green*) and anti-FLAG (*red*). *Left panels* are higher magnification views of the *boxed areas*. *Scale bar*, 10 μm. *J*, density of three-way junctions of the ER for cells examined as in *I*. Data are mean ± S.D. for 7 to 10 cells. *, $p < 0.05$ (one-way analysis of variance followed by Tukey's test). *K*, COS-7 cells transfected with expression vectors for tdTomato-tagged Sec61β and FLAG-tagged human protrudin (or with the corresponding empty vector, Mock) were treated (or not) with 100 μM nocodazole for 60 min to induce microtubule depolymerization. The cells were then fixed and processed for immunofluorescence analysis with anti-α-tubulin (*green*). The fluorescence of tdTomato was monitored directly. *Merged* images are also shown. The *boxed areas in the upper panels* are shown at higher magnification in the *lower panels*. *Scale bars*, 50 μm. The density of three-way junctions of the ER was also measured. Data are mean ± S.D. for three to seven cells. *, $p < 0.05$ (Student's *t* test).

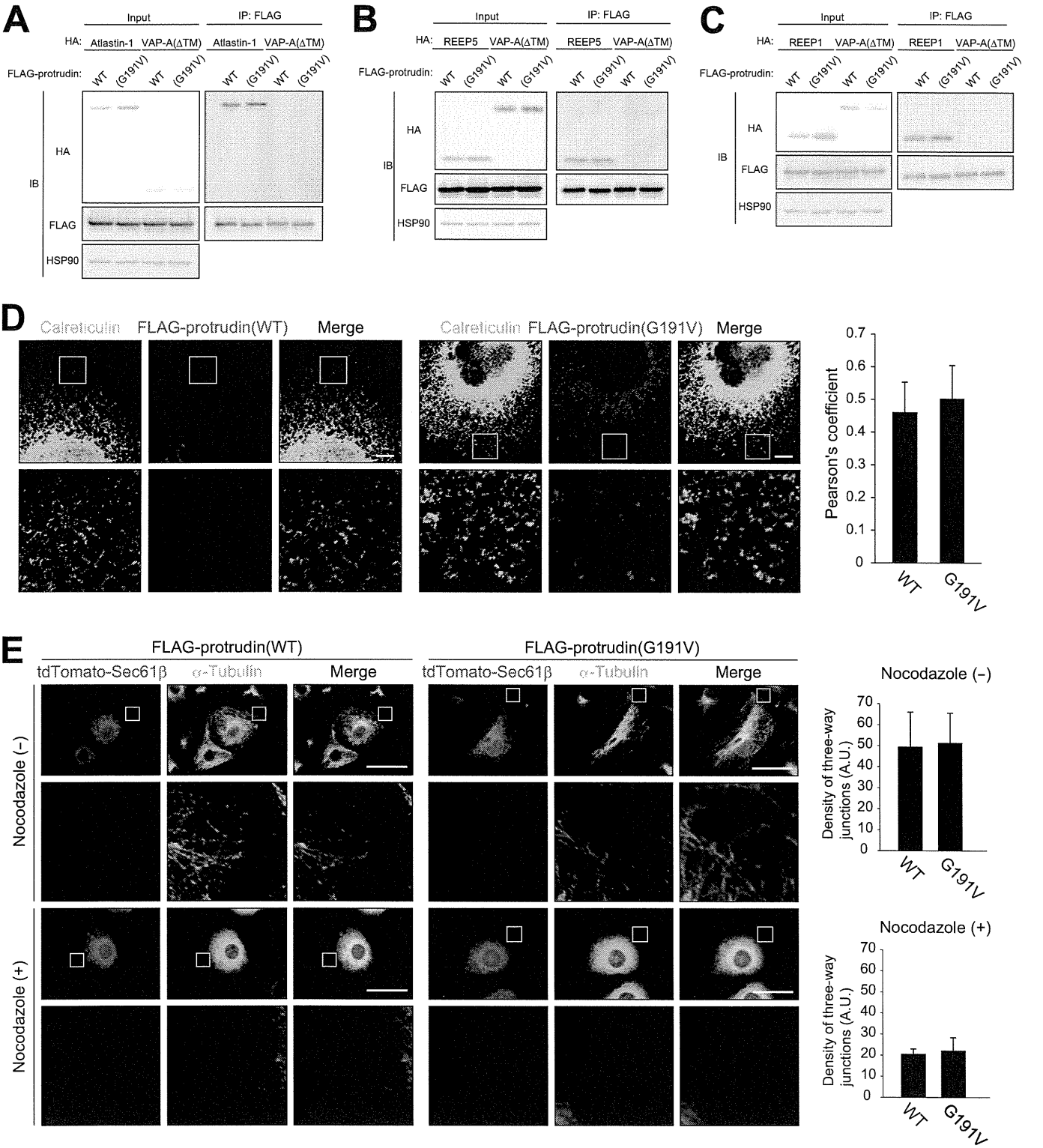

FIGURE 6. **An HSP-associated mutant of protrudin associates with atlastin-1 and REEP family members.** *A–C*, extracts of HEK293T cells transiently transfected with expression vectors for FLAG-tagged WT or G191V mutant forms of human protrudin as well as for HA epitope-tagged forms of atlastin-1, REEP5, or REEP1 were subjected to immunoprecipitation with anti-FLAG. VAP-A(ΔTM) was studied as a negative control for interaction with protrudin. The resulting precipitates, as well as a portion (1% of the input for immunoprecipitation) of the cell extracts, were subjected to immunoblot analysis with anti-HA, anti-FLAG, and anti-HSP90 (loading control). *D*, COS-7 cells expressing FLAG-tagged WT or G191V mutant forms of protrudin were fixed and processed for confocal immunofluorescence analysis with anti-calreticulin (*green*) and anti-FLAG (*red*). The *boxed regions of the upper panels* are shown at higher magnification in the *lower panels*. *Scale bars*, 10 μm. The percentage colocalization of FLAG-protrudin(WT) or FLAG-protrudin(G191V) with calreticulin was measured with Pearson's correlation coefficient in a square area of 2000 μm^2. Data are mean ± S.D. for four cells. *E*, COS-7 cells expressing tdTomato-tagged Sec61β and either FLAG-tagged protrudin(WT) or FLAG-protrudin(G191V) were treated (or not) with 100 μM nocodazole for 60 min. The cells were then fixed and processed for immunofluorescence analysis with anti-α-tubulin (*green*). The fluorescence of tdTomato was monitored directly. *Scale bars*, 50 μm. The density of three-way junctions of the ER was also measured. Data are mean ± S.D. for four or five cells.

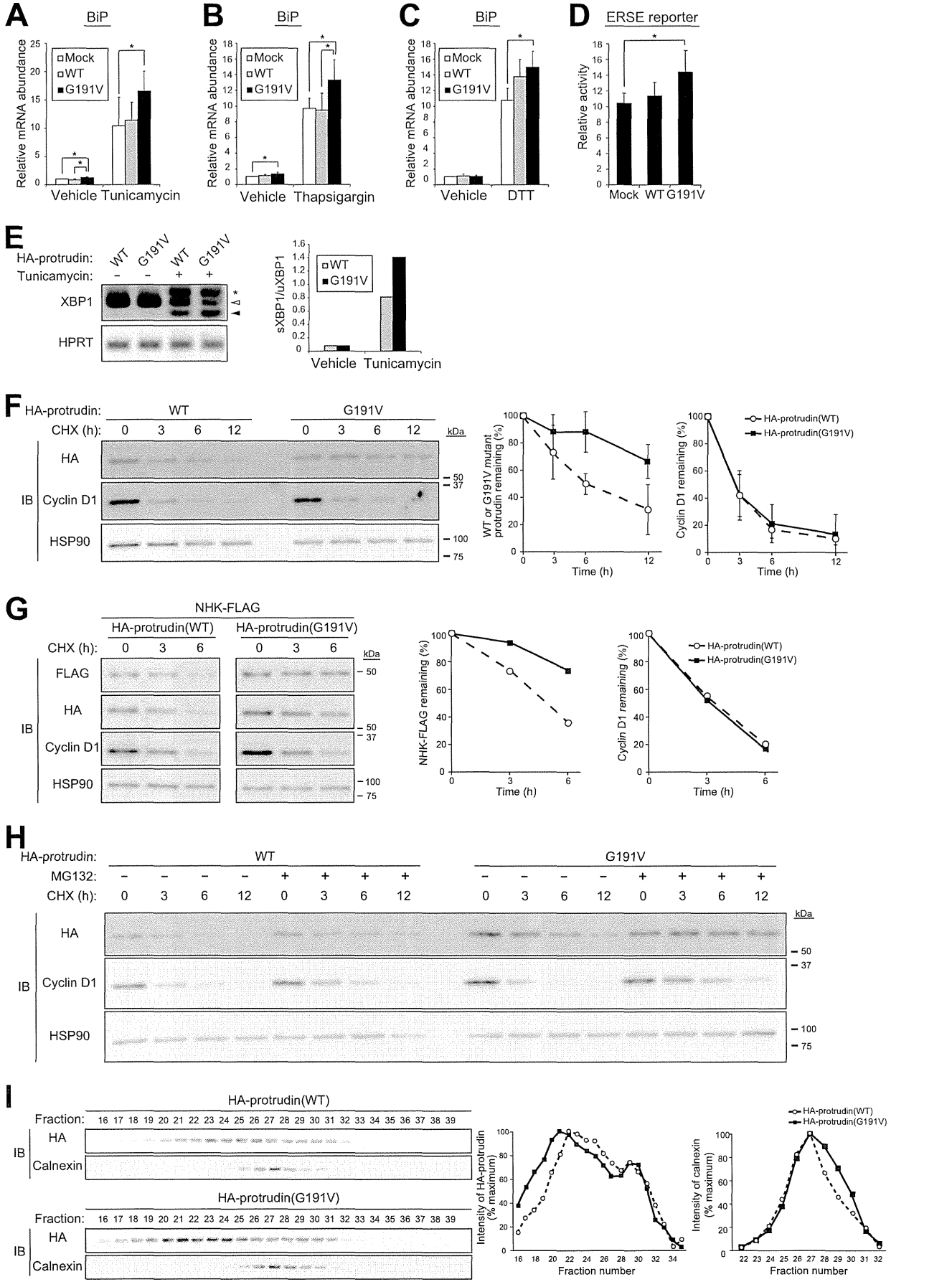
A
BiP
Relative mRNA abundance
Mock
WT
G191V
Vehicle
Tunicamycin
B
BiP
Thapsigargin
C
BiP
DTT
D
ERSE reporter
Relative activity
Mock WT G191V
E
HA-protrudin:
Tunicamycin:
XBP1
HPRT
sXBP1/uXBP1
F
HA-protrudin:
WT
G191V
CHX (h):
kDa
HA
IB
Cyclin D1
HSP90
WT or G191V mutant protrudin remaining (%)
Time (h)
HA-protrudin(WT)
HA-protrudin(G191V)
Cyclin D1 remaining (%)
G
NHK-FLAG
HA-protrudin(WT)
HA-protrudin(G191V)
FLAG
NHK-FLAG remaining (%)
H
MG132:
I
Fraction:
Calnexin
Intensity of HA-protrudin (% maximum)
Intensity of calnexin (% maximum)
Fraction number

largely responsible for the pathogenesis of HSP. Mutation of seipin (SPG17) has been shown to result in misfolding of the protein, aggregate formation, and ER stress, with these events likely playing a role in HSP pathogenesis (23, 28). Furthermore, the SPG18 protein Erlin2 has been functionally linked to ERAD (29). We have now shown that protrudin is localized predominantly to the tubular ER, and that expression of protrudin promotes formation of the tubular ER network.

Third, expression of the G191V mutant of protrudin rendered cells more vulnerable to ER stress, probably as a result of abnormal stability of the mutant protein. Glycine 191 is positioned in the hydrophobic hairpin domain of protrudin, and topology prediction *in silico* with the use of SOSUI software suggested that this mutation might result in a conformational change in the three-dimensional structure of protrudin, particularly in that of the FYVE domain, leading to misfolding of the COOH-terminal region (14). These results suggest that the G191V mutant of protrudin may be misfolded in the ER and therefore might stimulate the UPR.

We therefore conclude that protrudin shares common characteristics with other members of the SPG family: it interacts with other SPG proteins, harbors a hydrophobic hairpin domain, and regulates ER morphology. These characteristics suggest that, like other SPG proteins, protrudin contributes to ER network formation by regulating membrane curvature, and that mutation of protrudin is a causative defect in HSP. It is also possible that protrudin functions as a tethering factor through its FYVE domain, which is a lipid binding domain. EEA1, a typical FYVE-domain protein localized to early endosomes, possesses a structure similar to that of protrudin and serves as a tethering factor during fusion of early endosomes. Protrudin might thus function in cooperation with atlastin-1 to tether ER membranes for fusion during the formation of three-way junctions.

It remains unclear how protrudin links ER morphology and neuronal function. We previously showed that protrudin binds to Kif5 through its FFAT motif and coiled-coil domain, and that it serves as an adaptor protein to link the motor protein Kif5 and its cargo molecules including Rab11, VAP family members, and Surf4 (17). The protrudin-Kif5 complex contributes to the transport of these proteins in neurons and is essential for neurite elongation. The identification of mutations in the *KIF5A* gene in families with the SPG10 subtype of HSP has provided direct evidence for impairment of motor-based transport as an underlying cause of HSP (30). In mammals, the Kif5A motor protein mediates the anterograde transport of cargo such as vesicles along axons. Kif5 also regulates transport of cargo in dendrites and functions in several different membrane trafficking pathways. A VAP mutant that gives rise to familial ALS (ALS8) has been found to induce ER restructuring, providing further support for a role of aberrant ER morphogenesis in neurological disorders (31, 32). In addition, VAP contributes to tethering between the ER and the plasma membrane (33–35). Given that the UPR is activated in the ER of cells deficient in proteins that tether the ER to the plasma membrane, our results suggest that the protrudin-VAP interaction may play an integral role in regulation of ER morphology, function, and maintenance. The fact that several other HSP proteins also localize to the ER suggests that a fuller understanding of the function of these proteins may clarify the contribution of the ER to HSP pathogenesis. Further study of the pathological mechanisms of mutant forms of protrudin may lead to important new insights into motor neuron diseases, including other spastic paraplegias and ALS.

During preparation of the present manuscript, Chang *et al.* (36) described the interaction of protrudin with other HSP-related proteins in HEK293 cells (a human embryonic kidney cancer cell line) and a role for protrudin in the regulation of ER morphology. Although the results of the two independent studies overlap in part, we adopted a more physiological and comprehensive approach by applying proteomics analysis to neuron-specific protrudin transgenic mice. We thereby identified many HSP-related proteins as protrudin-interacting proteins in an unbiased manner. The detection of such interactions in mouse brain supports their physiological relevance. Furthermore, and most importantly, only our study includes characterization of a pathological mutant of protrudin(G191V) and provides insight into the pathogenesis of HSP caused by this mutation. The two studies performed independently and in parallel, however, reinforce and complement each other.

FIGURE 7. **Expression of an HSP-associated mutant of protrudin induces ER stress.** *A–C*, RT and real-time PCR analysis of BiP mRNA in Neuro2A cells infected with retroviruses encoding WT or G191V mutant forms of human protrudin and exposed to 5 μg/ml of tunicamycin (*A*), 1 μM thapsigargin (*B*), or 5 mM DTT (*C*) for 8 h. Data are expressed relative to the corresponding normalized value for cells infected with the empty retrovirus (*Mock*) and exposed to vehicle, and are mean ± S.D. from four to six independent experiments. *, $p < 0.05$ (one-way analysis of variance followed by Tukey's test). *D*, activity of an ER stress response element reporter plasmid relative to that of the reference plasmid pRL-TK in Neuro2A cells expressing WT or G191V mutant forms of protrudin. Data are mean ± S.D. from six independent experiments. *, $p < 0.05$ (one-way analysis of variance followed by Tukey's test). *E*, Neuro2A cells infected with retroviruses for HA epitope-tagged WT or G191V mutant forms of protrudin were incubated in the absence or presence of tunicamycin (2 μg/ml) for 7 h and then subjected to RT-PCR analysis of XBP1 mRNA and hypoxanthine-guanine phosphoribosyltransferase (*HPRT*) mRNA (loading control). *Open* and *filled arrowheads* indicate bands corresponding to unspliced (uXBP1) and spliced (sXBP1) forms of XBP1 mRNA, respectively. The *asterisk* indicates a nonspecific band. The sXBP1/uXBP1 band intensity ratio was measured. *F*, Neuro2A cells infected with retroviruses for HA epitope-tagged WT or G191V mutant forms of protrudin were incubated with cycloheximide (*CHX*, 10 μg/ml) for the indicated times, lysed, and subjected to immunoblot analysis with anti-HA, anti-cyclin D1 (positive control), and anti-HSP90 (loading control). The intensity of the HA-protrudin and cyclin D1 bands was measured. Data are mean ± S.D. for four independent experiments. *G*, Neuro2A cells infected with retroviruses for HA epitope-tagged WT or G191V mutant forms of protrudin were transfected for 48 h with a vector for FLAG-tagged NHK, incubated with cycloheximide (10 μg/ml) for the indicated times, lysed, and subjected to immunoblot analysis with anti-FLAG, anti-HA, anti-cyclin D1, and anti-HSP90. The intensity of the NHK-FLAG and cyclin D1 bands was measured. *H*, Neuro2A cells infected with retroviruses for HA epitope-tagged WT or G191V mutant forms of protrudin were incubated with cycloheximide (10 μg/ml) in the absence or presence of MG132 (10 μM) for the indicated times, lysed, and subjected to immunoblot analysis with anti-HA, anti-cyclin D1, and anti-HSP90. *I*, Neuro2A cells infected with retroviruses for HA epitope-tagged forms of WT or G191V mutant forms of protrudin were exposed to 1 μM thapsigargin for 8 h, lysed, and subjected to gel filtration chromatography with a running buffer containing 1% CHAPS. The resulting fractions were subjected to immunoblot analysis with anti-HA and anti-calnexin (negative control), and the intensity of the HA-protrudin and calnexin bands was measured. Similar results were obtained in two independent experiments.

Acknowledgments—We thank S. Nagata and H. Sumimoto for providing the pEFBOS-HHg vector; T. Kitamura for providing pMX-puro; H. Ichijo for providing pcDNA3-NHK-FLAG; K. Mori for providing pGL3-GRP78P(−132)-luc and p5×ATF6GL3; and A. Hamasaki and other laboratory members for technical assistance.

REFERENCES

1. Baumann, O., and Walz, B. (2001) Endoplasmic reticulum of animal cells and its organization into structural and functional domains. *Int. Rev. Cytol.* **205,** 149–214
2. Levine, T., and Rabouille, C. (2005) Endoplasmic reticulum: one continuous network compartmentalized by extrinsic cues. *Curr. Opin. Cell Biol.* **17,** 362–368
3. Ramírez, O. A., and Couve, A. (2011) The endoplasmic reticulum and protein trafficking in dendrites and axons. *Trends Cell Biol.* **21,** 219–227
4. Harding, A. E. (1983) Classification of the hereditary ataxias and paraplegias. *Lancet* **1,** 1151–1155
5. Finsterer, J., Löscher, W., Quasthoff, S., Wanschitz, J., Auer-Grumbach, M., and Stevanin, G. (2012) Hereditary spastic paraplegias with autosomal dominant, recessive, X-linked, or maternal trait of inheritance. *J. Neurol. Sci.* **318,** 1–18
6. Blackstone, C. (2012) Cellular pathways of hereditary spastic paraplegia. *Annu. Rev. Neurosci.* **35,** 25–47
7. Park, S. H., and Blackstone, C. (2010) Further assembly required: construction and dynamics of the endoplasmic reticulum network. *EMBO Rep.* **11,** 515–521
8. Park, S. H., Zhu, P. P., Parker, R. L., and Blackstone, C. (2010) Hereditary spastic paraplegia proteins REEP1, spastin, and atlastin-1 coordinate microtubule interactions with the tubular ER network. *J. Clin. Invest.* **120,** 1097–1110
9. Orso, G., Pendin, D., Liu, S., Tosetto, J., Moss, T. J., Faust, J. E., Micaroni, M., Egorova, A., Martinuzzi, A., McNew, J. A., and Daga, A. (2009) Homotypic fusion of ER membranes requires the dynamin-like GTPase atlastin. *Nature* **460,** 978–983
10. Hu, J., Shibata, Y., Zhu, P. P., Voss, C., Rismanchi, N., Prinz, W. A., Rapoport, T. A., and Blackstone, C. (2009) A class of dynamin-like GTPases involved in the generation of the tubular ER network. *Cell* **138,** 549–561
11. Hu, J., Prinz, W. A., and Rapoport, T. A. (2011) Weaving the web of ER tubules. *Cell* **147,** 1226–1231
12. Voeltz, G. K., Prinz, W. A., Shibata, Y., Rist, J. M., and Rapoport, T. A. (2006) A class of membrane proteins shaping the tubular endoplasmic reticulum. *Cell* **124,** 573–586
13. Anderson, D. J., and Hetzer, M. W. (2008) Reshaping of the endoplasmic reticulum limits the rate for nuclear envelope formation. *J. Cell Biol.* **182,** 911–924
14. Mannan, A. U., Krawen, P., Sauter, S. M., Boehm, J., Chronowska, A., Paulus, W., Neesen, J., and Engel, W. (2006) ZFYVE27 (SPG33), a novel spastin-binding protein, is mutated in hereditary spastic paraplegia. *Am. J. Hum. Genet.* **79,** 351–357
15. Shirane, M., and Nakayama, K. I. (2006) Protrudin induces neurite formation by directional membrane trafficking. *Science* **314,** 818–821
16. Saita, S., Shirane, M., Natume, T., Iemura, S., and Nakayama, K. I. (2009) Promotion of neurite extension by protrudin requires its interaction with vesicle-associated membrane protein-associated protein. *J. Biol. Chem.* **284,** 13766–13777
17. Matsuzaki, F., Shirane, M., Matsumoto, M., and Nakayama, K. I. (2011) Protrudin serves as an adaptor molecule that connects KIF5 and its cargoes in vesicular transport during process formation. *Mol. Biol. Cell* **22,** 4602–4620
18. Shirane, M., and Nakayama, K. I. (2003) Inherent calcineurin inhibitor FKBP38 targets Bcl-2 to mitochondria and inhibits apoptosis. *Nat. Cell Biol.* **5,** 28–37
19. Matsumoto, M., Oyamada, K., Takahashi, H., Sato, T., Hatakeyama, S., and Nakayama, K. I. (2009) Large-scale proteomic analysis of tyrosine-phosphorylation induced by T-cell receptor or B-cell receptor activation reveals new signaling pathways. *Proteomics* **9,** 3549–3563
20. Shibata, Y., Hu, J., Kozlov, M. M., and Rapoport, T. A. (2009) Mechanisms shaping the membranes of cellular organelles. *Annu. Rev. Cell Dev. Biol.* **25,** 329–354
21. Bian, X., Klemm, R. W., Liu, T. Y., Zhang, M., Sun, S., Sui, X., Liu, X., Rapoport, T. A., and Hu, J. (2011) Structures of the atlastin GTPase provide insight into homotypic fusion of endoplasmic reticulum membranes. *Proc. Natl. Acad. Sci. U.S.A.* **108,** 3976–3981
22. Anwar, K., Klemm, R. W., Condon, A., Severin, K. N., Zhang, M., Ghirlando, R., Hu, J., Rapoport, T. A., and Prinz, W. A. (2012) The dynamin-like GTPase Sey1p mediates homotypic ER fusion in *S. cerevisiae*. *J. Cell Biol.* **197,** 209–217
23. Yagi, T., Ito, D., Nihei, Y., Ishihara, T., and Suzuki, N. (2011) N88S seipin mutant transgenic mice develop features of seipinopathy/BSCL2-related motor neuron disease via endoplasmic reticulum stress. *Hum. Mol. Genet.* **20,** 3831–3840
24. Martignoni, M., Riano, E., and Rugarli, E. I. (2008) The role of ZFYVE27/protrudin in hereditary spastic paraplegia. *Am. J. Hum. Genet.* **83,** 127–128; author reply 128–130
25. Zhang, C., Li, D., Ma, Y., Yan, J., Yang, B., Li, P., Yu, A., Lu, C., and Ma, X. (2012) Role of spastin and protrudin in neurite outgrowth. *J. Cell Biochem.* **113,** 2296–2307
26. Shibata, Y., Voss, C., Rist, J. M., Hu, J., Rapoport, T. A., Prinz, W. A., and Voeltz, G. K. (2008) The reticulon and DP1/Yop1p proteins form immobile oligomers in the tubular endoplasmic reticulum. *J. Biol. Chem.* **283,** 18892–18904
27. Zhu, P. P., Soderblom, C., Tao-Cheng, J. H., Stadler, J., and Blackstone, C. (2006) SPG3A protein atlastin-1 is enriched in growth cones and promotes axon elongation during neuronal development. *Hum. Mol. Genet.* **15,** 1343–1353
28. Windpassinger, C., Auer-Grumbach, M., Irobi, J., Patel, H., Petek, E., Hörl, G., Malli, R., Reed, J. A., Dierick, I., Verpoorten, N., Warner, T. T., Proukakis, C., Van den Bergh, P., Verellen, C., Van Maldergem, L., Merlini, L., De Jonghe, P., Timmerman, V., Crosby, A. H., and Wagner, K. (2004) Heterozygous missense mutations in BSCL2 are associated with distal hereditary motor neuropathy and Silver syndrome. *Nat. Genet.* **36,** 271–276
29. Alazami, A. M., Adly, N., Al Dhalaan, H., and Alkuraya, F. S. (2011) A nullimorphic ERLIN2 mutation defines a complicated hereditary spastic paraplegia locus (SPG18). *Neurogenetics* **12,** 333–336
30. Reid, E., Kloos, M., Ashley-Koch, A., Hughes, L., Bevan, S., Svenson, I. K., Graham, F. L., Gaskell, P. C., Dearlove, A., Pericak-Vance, M. A., Rubinsztein, D. C., and Marchuk, D. A. (2002) A kinesin heavy chain (KIF5A) mutation in hereditary spastic paraplegia (SPG10). *Am. J. Hum. Genet.* **71,** 1189–1194
31. Nishimura, A. L., Mitne-Neto, M., Silva, H. C., Richieri-Costa, A., Middleton, S., Cascio, D., Kok, F., Oliveira, J. R., Gillingwater, T., Webb, J., Skehel, P., and Zatz, M. (2004) A mutation in the vesicle-trafficking protein VAPB causes late-onset spinal muscular atrophy and amyotrophic lateral sclerosis. *Am. J. Hum. Genet.* **75,** 822–831
32. Marques, V. D., Barreira, A. A., Davis, M. B., Abou-Sleiman, P. M., Silva, W. A., Jr., Zago, M. A., Sobreira, C., Fazan, V., and Marques, W., Jr. (2006) Expanding the phenotypes of the Pro56Ser VAPB mutation: proximal SMA with dysautonomia. *Muscle Nerve* **34,** 731–739
33. Loewen, C. J., Young, B. P., Tavassoli, S., and Levine, T. P. (2007) Inheritance of cortical ER in yeast is required for normal septin organization. *J. Cell Biol.* **179,** 467–483
34. Stefan, C. J., Manford, A. G., Baird, D., Yamada-Hanff, J., Mao, Y., and Emr, S. D. (2011) Osh proteins regulate phosphoinositide metabolism at ER-plasma membrane contact sites. *Cell* **144,** 389–401
35. Manford, A. G., Stefan, C. J., Yuan, H. L., Macgurn, J. A., and Emr, S. D. (2012) ER-to-plasma membrane tethering proteins regulate cell signaling and ER morphology. *Dev. Cell* **23,** 1129–1140
36. Chang, J., Lee, S., and Blackstone, C. (2013) Protrudin binds atlastins and endoplasmic reticulum-shaping proteins and regulates network formation. *Proc. Natl. Acad. Sci. U.S.A.* **110,** 14954–14959